

Mechanosensitive Closed-Closed Transitions in Large Membrane Proteins: Osmoprotection and Tension Damping

Pierre-Alexandre Boucher,[†] Catherine E. Morris,[‡] and Béla Joós^{†*}

[†]Institut de Physique, Ottawa-Carleton Campus de l'Université d'Ottawa, Ottawa, Ontario, Canada; and [‡]Neurosciences, Ottawa Health Research Institute, Ottawa, Ontario, Canada

ABSTRACT Multiconformation membrane proteins are mechanosensitive (MS) if their conformations displace different bilayer areas. Might MS closed-closed transitions serve as tension buffers, that is, as membrane “spandex”? While bilayer expansion is effectively instantaneous, transitions of bilayer-embedded MS proteins are stochastic (thermally activated) so spandex kinetics would be critical. Here we model generic two-state (contracted/expanded) stochastic spandexes inspired by known bacterial osmovalves (MscL, MscS) then suggest experimental approaches to test for spandex-like behaviors in these proteins. Modeling shows: 1), spandex kinetics depend on the transition state location along an area reaction coordinate; 2), increasing membrane concentration of a spandex right-shifts its midpoint (= tension-Boltzmann); 3), spandexes with midpoints below the activating tension of an osmovalve could optimize osmovalve deployment (required: large midpoint, barrier near the expanded state); 4), spandexes could damp bilayer tension excursions (required: midpoint at target tension, and for speed, barrier halfway between the contracted and expanded states; the larger the spandex Δ -area, the more precise the maintenance of target tension; higher spandex concentrations damp larger amplitude strain fluctuations). One spandex species could not excel as both first line of defense for osmovalve partners and tension damper. Possible interactions among MS closed-closed and closed-open transitions are discussed for MscS- and MscL-like proteins.

INTRODUCTION

Multiconformation membrane proteins whose states displace different bilayer areas make mechanosensitive (MS) transitions between those states (1). Not surprisingly, such proteins occur in all organisms (1–4). Since bilayer strain >3–4% quickly leads to rupture (5), cells might use large Δ -area MS membrane proteins as tension buffers (Fig. 1, A and B). Large Δ -area (>100% range) membrane proteins occur in high-turgor walled prokaryotes and are osmoprotective (3). Here we consider, on theoretical grounds, direct tension buffering by MS membrane proteins. Theory developed for eukaryotic cells suggests how irreversible (plastic) tension buffering could be achieved from folded membrane (e.g., caveolae, filopodia) (6), but there is no equivalent theory for reversible (elastic) membrane tension buffering by tension-gated membrane proteins. Inspired by the characteristics and expression levels of bacterial osmovalves, we have postulated (7) that populations of membrane proteins with MS closed-closed transitions could operate as stochastic membrane spandex—i.e., as stretch-gated tension buffers. Specifically, it was MscL with its MS preopening expansion transition (8) and its apparent overexpression of ~60/cell (B. Martinac, personal communication, 2009; and reported in 1997 as ~50 channels/cell (10)) that inspired the idea. MscS family proteins too may have MS closed-closed transitions. Here we generate a simple energetic and dynamical theory for membrane spandex, and suggest several ways to

investigate whether MS bacterial membrane proteins operate as tension buffers.

Bacterial osmotic valve proteins

The best-characterized MS membrane proteins are bacterial MscL, MscS, and their homologs (3,4). Both multimers expand to form nonselective channels that serve as emergency osmovalves (3). Valve opening at slightly sublytic tensions (e.g., (11, 12)) releases osmolytes and water, reducing cell volume, wall distension, and bilayer tension (3,13). Although the benefits of valve opening are clear, so are the costs: loss of expensive osmolytes and, at low pH, exposure of cytoplasm to potentially lethal acidification (14). MscL, e.g., releases osmolytes up to 400–500 kDa. However, recognizing acceptable tension noise, saving valve opening for truly catastrophic perturbations, would seem a desirable general strategy.

Why do bacteria express multiple copies of MscL and MscS per cell? MscS expands at tensions substantially lower than MscL. Why? Estimates of MscL channels/cell differ by an order of magnitude (i.e., ~5–~50) (10,15), but even at the low end, the entire MscL/MscS collection would seem excessive for emergency osmolyte release. A single stretch-activated MscL (~1 nS unitary conductance, $P_{\text{open}} \sim 1$ at near-lytic tensions (16)) should suffice. With its large pore size (a 25 Å cylinder of radius 12.5 Å (17)), one open MscL could relieve tension in a bacterium exposed to pure water, yielding a safe pressure differential (<0.4 Osm (15)) within ~0.55 s. This time course assumes exponential decrease of cytoplasmic osmolytes via a channel with efflux characteristics as per

Submitted June 1, 2009, and accepted for publication August 31, 2009.

*Correspondence: bjoos@science.uottawa.ca

Editor: Reinhard Lipowsky.

© 2009 by the Biophysical Society
0006-3495/09/11/2761/10 \$2.00

doi: 10.1016/j.bpj.2009.08.054

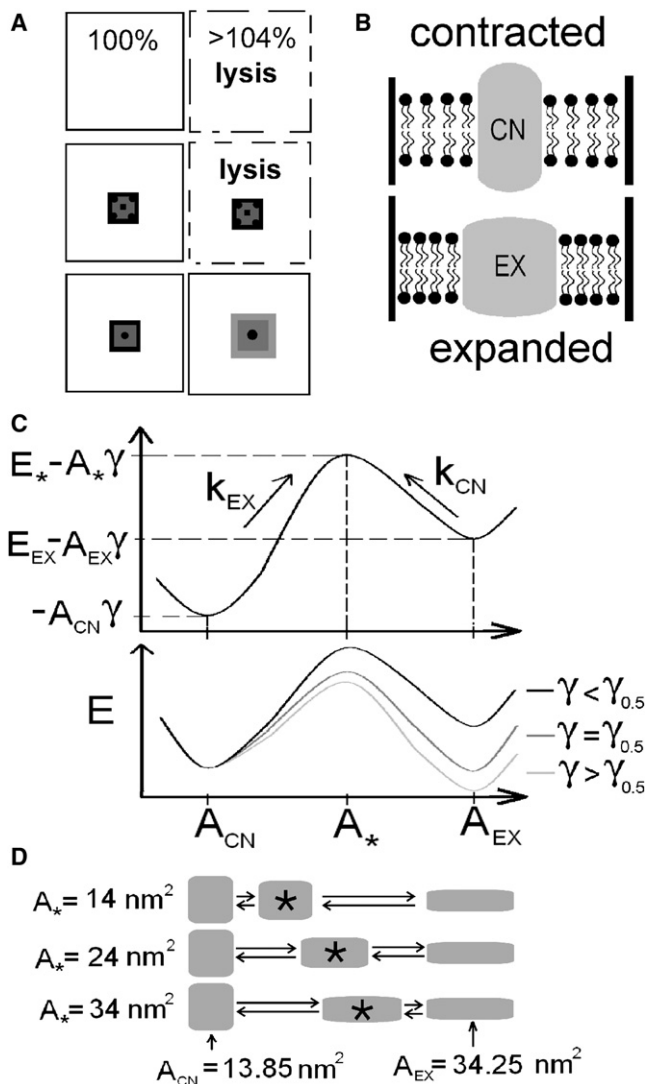


FIGURE 1 (A) Pure lipid bilayers (top), or ones with nonexpanding proteins (middle), rupture (i.e., lyse) under strain $\sim 4\%$, whereas expanding proteins (bottom) could prevent lysis by relief of tension. (B) The spandex model states (contracted, CN; expanded, EX). For a given strain, bilayer tension ($= \gamma$) is higher with CN than with EX. (C) Spandex energy landscapes (reaction coordinate: protein area). (Top) A landscape for $\gamma < \gamma_{0.5}$, the spandex midpoint tension, illustrates the model's parameters: A_{CN} , A_* , and A_{EX} are the areas associated with the CN, transition (barrier) and EX states. With CN taken as the reference state, E_* and E_{EX} are the energies of the barrier state and of EX. k_{EX} and k_{CN} are the transition rates. (Bottom) As bilayer tension increases, the energy of the EX and barrier states decrease linearly, relative to CN. At $\gamma = \gamma_{0.5}$ CN and EX have the same energy and the probabilities of being expanded and contracted (P_{EX} , P_{CN}) are equal. (D) Three spandex proteins with different values for A_* (the transition energy maximum's position) and with A_{CN} and A_{EX} fixed at values reported for MscL (17).

Eq. 11-6 in Hille (18) (cytoplasmic [osmolyte] = 1 M, bacterial volume = 10^{-15} l, diffusion constant = 1.5×10^{-9} m²/s). Bacterial protoplasts rupture at ~ 10 mN/m. Dynamic tension spectroscopy (5) shows that bilayers rupturing in that range (8–9 mN/m) are safe for ~ 100 s under low-to-moderate bilayer strain rates (~ 1 mN/m/s), and that for strain rates

~ 100 -fold faster, the same bilayer ruptures at tensions twofold higher. This suggests that during turgor upsurges, a population of MscL with a closed-closed expansion en route to opening could obviate the need to use the valve.

In addition to multiple copies of MscL and MscS, bacteria express MscS homologs whose expression increases when conditions demand osmoprotection (3). Viability assays plus electrophysiological and biochemical analysis reveal that in exponential and stationary phase growth, *Escherichia coli* deploys 10–15 and 20–30 copies, respectively, of MscS/cell, with growth at high osmolarity further increasing MscS density (15). Could the excess have nonvalve mechanoprotective roles? MscS channels can enter a nonconducting expanded state (19); in vitro, this occurs from the open state, but in vivo conditions might favor direct transition from closed (CN) to inactivated (EX) as seen in vitro for an MscS point mutant (20). A fast open-inactivated transition (< 1 ms range) in vivo might achieve almost the same effect, while also providing minor osmotic relief. The notion of MscS having an EX state with little or no associated flux seems especially plausible, given that a handful of MscS homologs (3), by patch clamp, are electrically silent. Such silent EX states in either osmolyte proteins or in coexpressed proteins might serve as a first line of defense to relax bilayer tension while retaining valuable osmolytes.

We develop a two-state model directly comparable to stochastic two-state models for ligand-, voltage-, and mechanically gated channels: spandex transitions occur across energy barriers small enough to be surmounted by thermal energy, with the gating free energy linearly dependent on membrane tension (21). Within that context, we ask what design features of spandex proteins might allow them to act as tension relievers.

Bilayer tension fluctuations in walled cells

Surprisingly little information is available on the mechanical interplay of cell wall and lipid bilayer, an interaction highly relevant to bilayer tension and hence to MS gating of bilayer-embedded bacterial proteins. Area compressibility can be directly assessed for unsupported bilayers (22), but not for complex bilayers supported by cell walls. Nevertheless, when turgor presses bacterial bilayers against the mechanically supportive peptidoglycan cell wall (23), bilayer tension must change in concert with any wall compressibility changes such as those due to exterior and interior environment pH variations (24).

Osmo-metabolite fluctuations will also generate bilayer tension fluctuations. Consider bacteria-sized spherical vesicle of radius = $1 \mu\text{m}$ in a 1 M isotonic solution at 300 K and suppose a single additional osmolyte (plus osmotically obliged water) appears inside the vesicle. At a typical bilayer compressibility of 235 mN/m (22), the resulting tension increase is 0.235×10^{-6} mN/m per osmolyte. A $\pm 4\%$ fluctuation in [osmolyte] would correspond at 1 M ($\sim 10^8$ osmolytes)

to a ± 1 mN/m tension fluctuation (= 1/8 times the osmovalve midpoint tension); depending on load-sharing between bilayer and wall under the prevailing conditions, this might gate an osmovalve.

In walled (i.e., elevated turgor pressure) nanomechanical motions, as measured in yeast (25), may also be relevant there. The ATP- and temperature-dependent periodic nanomechanical motions (~ 3 nm, 0.8–1.6 kHz), thermodynamic characteristics, and force magnitude (~ 10 nN) suggest concerted myosin-type action. If force associated with the motion distributed itself over the entire plasma membrane, bilayer tension (assuming spherical geometry) would be 2×10^{-4} mN/m (= 0.25×10^{-4} times the osmovalve midpoint tension). Several simultaneous motions might generate tension noise (above the turgor background) sufficient to mistrigger an osmotic valve. It is worth noting that bacteria, too, possess dynamic (proto)cytoskeletons (26).

MS closed-closed transitions in various proteins

As noted above, electrophysiological and structural indications for MscS (20) and MscL (27) (and mutants) point to MS closed-closed transitions, preopen EX states in the activation path, or to closed-inactivated EX states. Its preopening transition may expand MscL to $\sim 80\%$ of its open area, the remaining 20% occurring on pore opening (8). MscS opens directly from the closed state, but under sustained tension, inactivates, possibly enlarging further (20). Additionally, if, in situ, some MscL and MscS multimers were occluded when open (both possess elaborate cytoplasmic filters), this would let them act as spandexes.

Eukaryotic cells also have spandex candidates. Prestin, described as a piezoelectric device (e.g., (28)) would be a “voltage-activated spandex”. Changes of the in-plane area of this outer hair cell membrane proteins (99 nm^2 (29) when contracted), which occupies $\sim 60\%$ of the membrane (30), alter the cell’s dimensions (28,31). Its MS transition would need to be described along at least two reaction coordinates (i.e., area and charge displacement) (32). The length-scale of prestin’s piezoelectric transition is of the same order as for other MS proteins (8.4 nm^2 for MscS (19), 4 nm^2 for prestin (30)). In Kv1-type (*Shaker*) channels, atomic-force microscopy (AFM) evidence shows that voltage sensor transitions affect membrane electromotility (33), likely reflecting lateral interactions between protein and lipid bilayer, a not-unexpected finding given the MS activation kinetics of *Shaker* (e.g., (34)). Kinetic interplay between two species of piezoelectric MS proteins may develop when fast-gating Kv channels optimize prestin mechanics (35). Photodetecting rhodopsin occurs at $25,000 \mu\text{m}^{-2}$ in rod outer segment membrane (36), i.e., $\sim 35\%$ surface occupancy given its in-plane area (15 nm^2 (37)). Since photoactivation causes an estimated 1.3 nm^2 (38) area change, simultaneous photoactivation of all the rhodopsins must perturb bilayer tension; coembedded membrane proteins would “feel” the event.

Here, using MscL-like and MscS-like values, we generate a prototype model for membrane proteins with expanding closed-closed transitions. Our two-state (CN/EX) protein has an activation barrier on a single reaction coordinate: spandex area in the plane of the bilayer. The barrier position along this axis proved critical to spandex transition kinetics. Modeling the transition as solely tension-dependent is a useful simplification but ignores other possible energy dependences. In reality, multiple sources of energy may contribute and accordingly, multiple reaction coordinates would pertain, with barriers to expansion along those reaction coordinates (21,32), as with voltage-gated proteins modulated by tension (39,40). In much the same way, energy arising from the height difference between a spandex and the lipid bilayer (hydrophobic mismatch) would be another reaction coordinate. The model implicitly includes this free energy in E_{EX} , the energy difference between the reference (CN) and expanded (EX) states. Wiggins and Phillips (41,42) calculated gating energetics for a MscL-like MS protein embedded in a lipid bilayer and found the major contribution to be the protein’s areal deformation.

Our model differs from this and other models that focus on the individual-molecule traits of an MS protein (e.g., molecular dynamics simulations). We assign individual protein properties then explore how the MS protein behaves as part of a population; kinetics (not equilibrium energetics) is the issue of central interest. In a recent overview, Phillips et al. (43) indicated that isolated versus densely-packed MS proteins will exhibit different behaviors. They examined the pairwise energetic interactions of close-proximity MS proteins (44) but not population behaviors.

Because 1), the membrane spandex idea was inspired by the large Δ -area osmovalves (channels whose opening could trump any other MS transition); and 2), there is straightforward biological relevance and experimental potential in bacterial systems, we specified that spandex transitions are ones involving no fluxes. However, in other systems, potentially dangerous fluctuations of bilayer tension might be driven not osmotically but strictly mechanically (e.g., cells strained by erratic shear flow). There, other classes of Δ -area transitions—perhaps even MS open-open transition—might serve as spandex transitions. In circulating erythrocytes, for instance, some of the abundant transport proteins might take part-time jobs as spandex.

MODELING

Sukharev et al. (27) and Sukharev and Markin (45) described the opening (and expansion, as in our case) of a MS protein in terms of opening and closing rates. A similar method is used here. A spandex membrane protein is considered to be a two-state protein (Fig. 1 B). The states, neither of which supports a flux, are contracted (CN) and expanded (EX). There is a transition or barrier state where the energy of the protein is at a maximum E_* (27). A typical plot of the

variation of the enthalpy of the spandex as a function of its area is shown in Fig. 1 C, where γ is bilayer tension. Using this energy landscape, the expansion k_{EX} and contraction k_{CN} rates can be written as

$$\begin{aligned} k_{EX} &= k_0 \exp((-E_* + (A_* - A_{CN})\gamma)/k_B T_r) \\ k_{CN} &= k_0 \exp((-E_* + E_{EX} - (A_{EX} - A_*)\gamma)/k_B T_r), \end{aligned} \quad (1)$$

where k_0 is the attempt rate taken as equal for both transitions to preserve detailed balance, and E_* and E_{EX} are, respectively, the barrier and the EX state energy with respect to the CN state. A_{CN} , A_* , and A_{EX} are the areas of the three states. $k_B T_r$ is the room temperature energy per particle. The rate of change of occupancy of the expanded state is

$$\frac{dP_{EX}}{dt} = -k_{CN}P_{EX} + k_{EX}(1 - P_{EX}), \quad (2)$$

where P_{EX} is the probability for a protein to be in the EX state. The corresponding probability for the CN state is given by $P_{CN} = 1 - P_{EX}$. The equilibrium (i.e., infinite time) solution of Eq. 2 is

$$P_{EX} = \frac{k_{EX}}{k_{EX} + k_{CN}}, \quad (3)$$

and does not depend on E_* , k_0 , or A_* .

Expanded proteins occupy more space in the plane of the bilayer, reducing both the area available for lipids and bilayer tension. Considering the stress-strain relation in a lipid bilayer ($\gamma = K\Delta a/a_0$), where $\Delta a/a_0$ is the strain on the lipid bilayer and K is the compressibility modulus of the lipid bilayer; and substituting for the relative area increase in a similar way as in the literature (6,46),

$$\gamma = K \frac{\Delta a_m}{a_m} - \frac{K\Delta A C_{prot}}{A_{CN}} P_{EX}, \quad (4)$$

where $\Delta a_m/a_m$ is the strain imposed on the whole system (i.e., lipid bilayer + spandex proteins) and ΔA is the spandex area change ($= A_{EX} - A_{CN}$). $\Delta a_m/a_m$ is independent of the proteins and should be seen as a relative area change induced, e.g., by osmotic swelling. The last term in Eq. 4 corresponds to the relaxation of the bilayer due to spandex expansion. The protein concentration, C_{prot} , is defined as the ratio of the area occupied by contracted spandexes to the total area of the system. Taking the derivative of Eq. 4 with respect to time:

$$\frac{d\gamma}{dt} = K \frac{d}{dt} \frac{\Delta a_m}{a_m} - \frac{K C_{prot} \Delta A}{A_{CN}} \frac{dP_{EX}}{dt}. \quad (5)$$

The quantity $K\Delta a_m/a_m$ is the tension felt by a pure bilayer or a bilayer with nonexpansible proteins and will be used to express strains in accessible units.

The tension at which half of the spandex proteins are in the expanded state at equilibrium is called the midpoint, $\gamma_{0.5}$ (Fig. 1 C, bottom). The relation among $\gamma_{0.5}$, ΔA , and E_{EX} ,

$$\gamma_{0.5} = \frac{E_{EX}}{\Delta A}, \quad (6)$$

is obtained by setting equal the rates in Eq. 1.

The spandex time constant, τ_{prot} , is the characteristic time needed to reach the P_{EX} value associated with the tension, and is given by

$$\tau_{prot} = \frac{1}{k_{EX} + k_{CN}}. \quad (7)$$

The τ_{prot} is a function of A_* , k_0 , and E_* as well as of ΔA and E_{EX} .

Values for the constant parameters are $k_B T_r = 4.04$ pN nm (corresponding to 23°C) and $K = 235$ mN/m (22). $A_{CN} = 13.85$ nm² and ΔA to 20.4 nm² (similar to MscL (17)) are used unless stated otherwise. E_{EX} is set through Eq. 6 by setting the midpoint $\gamma_{0.5} = 8$ mN/m (slightly lower than the lytic tension of bacterial and spheroplast bilayers). The values k_0 and E_* , although not independent parameters, are adjusted to have a maximum value of the time constant $\tau_{max} = 5$ ms, the same order of magnitude as the time constant for the opening of MscL (16). These values are used unless stated otherwise. The parameters left to vary are A_* , C_{prot} , and $\Delta a_m/a_m$, which may be a function of time, depending on the type of simulation. The model is solved numerically: at every timestep, the values of P_{EX} and γ are computed by using Eqs. 2 and 5, respectively.

One spandex in a large bilayer (i.e., isolated protein) would not affect bilayer tension. The $C_{prot} = 0$ condition, simulating vanishingly small levels of spandex, is used here when characterizing a spandex's fundamental properties.

Except for tension relaxation, the model ignores bilayer-mediated protein-protein interactions such as those occurring at short-range due to thickness or midplane deformations (40,42). Assuming that short-range means $<3 \times$ the protein's radius (43), the maximum C_{prot} our model can handle is $\sim 10\%$ for a protein the size of MscL.

The finite stiffnesses of spandex states would displace energy minima and maximum when bilayer tension changed; ignoring this detail makes the independent analysis of kinetically relevant parameters clearer (see Supporting Material).

PROTEIN CHARACTERISTICS

Isolated protein characteristics

To understand membrane spandex populations, we first need to characterize, for different spandexes, isolated spandex behavior under stress. An important spandex parameter is area change upon expansion, ΔA , which directly impacts spandex tension sensitivity (Fig. 2 A). Even proteins not considered mechanosensitive per se, but having a small ΔA (in the 1 nm² range, e.g., rhodopsin and some voltage-gated channels) would be tension-modulated. A large ΔA makes the transition very abrupt with tension as seen in Fig. 2 A.

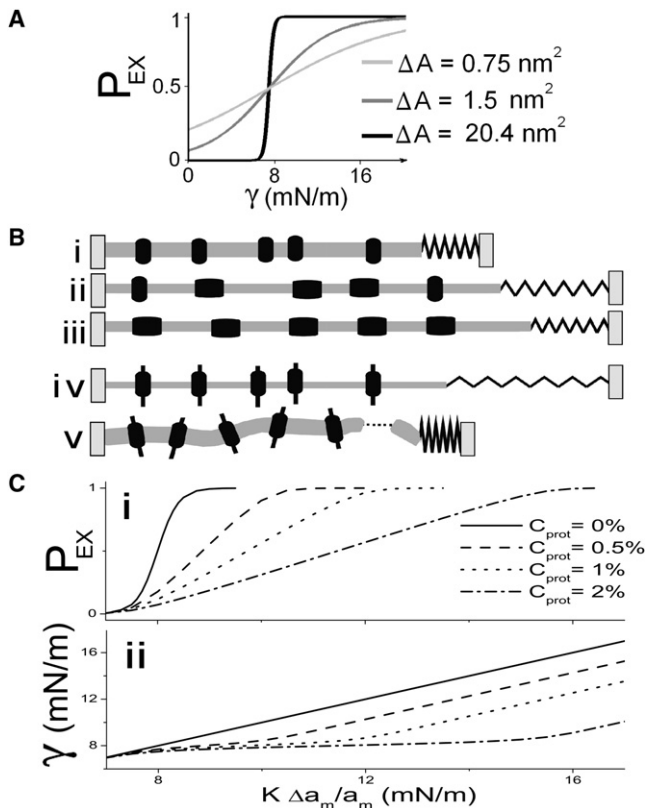


FIGURE 2 (A) $P_{EX}(\gamma)$ (i.e., tension-Boltzmanns) for three different ΔA spandexes with the same midpoint at 8 mN/m (i.e., slightly lower than that for MscL). $\Delta A = 0.75 \text{ nm}^2$ could be any generic small ΔA protein; $\Delta A = 1.5 \text{ nm}^2$ is in the range calculated for KvAP activation (38); and $\Delta A = 20.4 \text{ nm}^2$ corresponds to MscL (17). (B) A mildly stressed membrane with contracted spandex proteins (i) that is suddenly exposed to a large strain (due, say, to high turgor) (ii) will experience elevated bilayer tension (the spring length, γ , increases) that progressively falls as more spandex proteins expand (iii). If the membrane contained exclusively nonexpansible proteins (iv) it would be more likely to rupture (v). (C) The effect of spandex concentration, C_{prot} , on P_{EX} (i), and on γ (ii), as a function of imposed strain (multiplied by bilayer compressibility: $K\Delta a_m/a_m$). (i) Shows the P_{EX} midpoint right-shifting and (ii) shows bilayer tension flattening with increasing C_{prot} .

What constitutes the optimal value of ΔA for a good anti-rupture spandex? Such a spandex needs to remain contracted, except when tension reaches values dangerous for the integrity of the lipid bilayer. A ΔA as large as feasible is called for. Very large proteins could be costly or risky to produce error-free, but the limit is set by metabolism, not by the physics of spandex. The advantage offered by a large ΔA spandex, as we show in the next subsection, can be equaled by a larger concentration of a smaller spandex (albeit not so small as to make it tension-insensitive).

Characteristics of a population of proteins

Spandex transition rates in the model depend only on bilayer tension. This tension is, however, relaxed by the expanding spandex proteins (Fig. 2 B). The level of strain required to expand half a spandex population is calculated by setting

$P_{EX} = 1/2$ and $dP_{EX}/dt = 0$, and using Eq. 4 to obtain the relation

$$\gamma_{0.5pop} = \gamma_{0.5} + \frac{KC_{prot}\Delta A}{2A_{CN}}, \quad (8)$$

where $\gamma_{0.5pop}$ is the imposed strain (multiplied by the compressibility = $K\Delta a_m/a_m$) at which half the proteins are in the expanded state. The value $\gamma_{0.5pop}$ depends on [spandex].

In Fig. 2 C i, the slope of P_{EX} becomes shallower with increasing C_{prot} giving the appearance of a smaller ΔA spandex with a higher midpoint. However, this figure can be misleading because P_{EX} alone does not give a good idea of bilayer tension. Fig. 2 C ii plots bilayer tension versus imposed strain for several C_{prot} . Below the spandex's midpoint tension, curves superpose but approaching the midpoint (8 mN/m), they start diverging as spandex expansion stabilizes bilayer tension relative to imposed strain.

Position of the transition barrier

The value of A^* is of central importance to the kinetics of a spandex protein. When A^* is close to A_{CN} , the exponent for k_{EX} in Eq. 1 becomes small making k_{EX} a weak function of γ . At high tensions, the closing rate, k_{CN} , becomes very small due to its exponential dependence on γ leaving the time constant (Eq. 7) dominated by k_{EX} . Thus at large tensions, the time constant becomes a weak function of tension, as seen in Fig. 3 A. Similar reasoning applies where A^* is close to A_{EX} (Fig. 3 C). When A^* is midway between A_{CN} and A_{EX} , the time constant is symmetric in γ above and below the threshold (Eq. 1).

A spandex designed to prevent bilayer rupture would need to react fast when tension increased to near the bilayer's lytic value, but need not be particularly fast at lower tension. So a spandex with a large value of A^* would be appropriate (Fig. 4 A). To maintain a fixed bilayer tension, a spandex would need to expand fast when tension rises, and contract equally fast when tension decreases. Here, a barrier located halfway between EX and CN states would be optimal. A protein that needed to avoid interference from tension fluctuations above its midpoint could achieve that by having a small A^* .

Given the importance of A^* , it would interesting to know what controls its value. Can the transition barrier be displaced, and if so, can a spandex protein be controlled such that it would act as a good tension reliever in one set of conditions and a good tension damper in another set of conditions?

TENSION DAMPING

Cell membranes are subjected to time-varying strains due to fluctuations in osmotic and hydrostatic pressures and adhesion strengths, plus, for walled high turgor cells, to variations in cell wall elasticity. Could spandex proteins serve to maintain bilayer tension within a given range (if/when it was

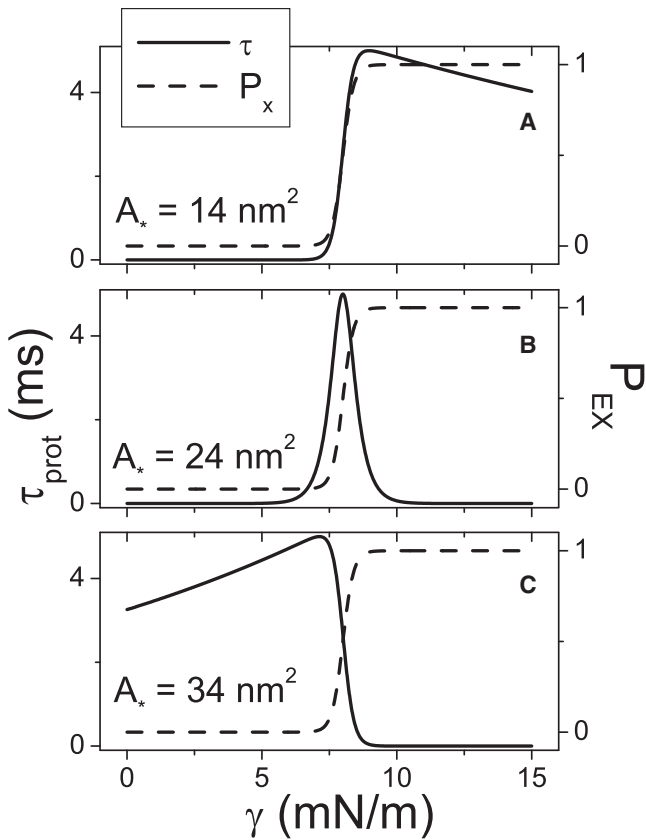


FIGURE 3 For an isolated spandex protein ($C_{\text{prot}} = 0$), varying barrier location, A_* , changes the tension-dependence of τ_{prot} (the protein time constant, from Eq. 7) (solid lines) without changing the tension-dependence of P_{EX} (from Eq. 3) (dashed lines).

advantageous for stretch-modulated membrane proteins to operate within a particular tension range)? To simulate the reaction of spandex protein to random strains, strain was varied as a sine wave. In Eq. 4, we put $\Delta a_m/a_m = \text{Amp}[\sin(2\pi t/T)]$, where t is time and T is the period.

For optimal tension damping, a spandex protein must expand to relieve bilayer tension as it increases above a certain target value γ_0 and contract to increase tension as it decreases below that value. A spandex protein's midpoint ($\gamma_{0.5}$) must hence equal γ_0 (arbitrarily 8 mN/m in this work). The goal is to maintain the system in the flat section of Fig. 2 C ii, where strain can vary, but tension is kept almost constant. The flat region increases with the density of spandexes. This region is centered at the spandex population midpoint $\gamma_{0.5\text{pop}}$ (Eq. 8) where $P_{\text{EX}} = 0.5$ in the P_{EX} versus applied strain curve (Fig. 2 C, i and ii).

It would take a spandex of arbitrarily large ΔA to keep bilayer tension constant; its P_{EX} would be unity above the midpoint, and 0 below. For finite values of ΔA , tension will change around the target tension because the expansion probability on either side of the midpoint is not infinitely steep with tension (Fig. 2 A).

For a spandex to be a good tension damper, expansion and contraction transitions must be equally dependent on tension,

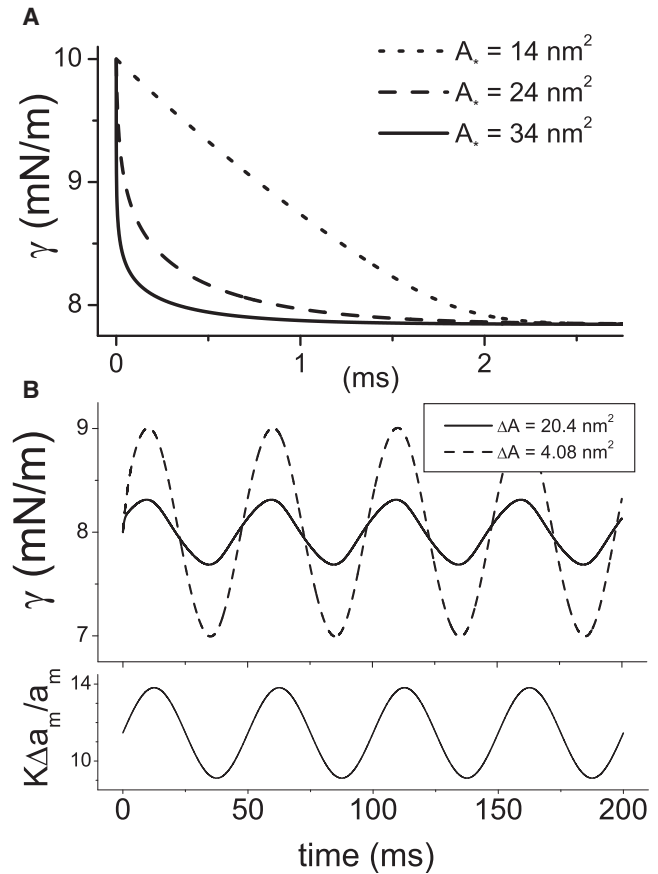


FIGURE 4 (A) Spandexes with different A_* values but otherwise identical parameters ($\gamma_{0.5}$, ΔA , τ_{max} , C_{prot} , etc.) relieve tension with different speeds. The time course of bilayer tension after a step strain at $t = 0$ (0–4.26%) ($K\Delta a_m/a_m = 0$ –10 mN/m) is plotted for three different A_* spandexes ($C_{\text{prot}} = 2\%$); though all three have the same τ_{max} , they have different $\tau(\gamma)$ behavior (Fig. 3). (B) Two different spandex proteins serve to damp bilayer stress (top) under oscillatory strain (bottom). Damping quality depends on the spandex ΔA . C_{prot} is varied to keep the product ΔAC_{prot} constant: $\Delta A = 20.4 \text{ nm}^2$ and $C_{\text{prot}} = 0.02$ (solid line) and $\Delta A = 4.08 \text{ nm}^2$ and $C_{\text{prot}} = 0.1$ (dashed line). The strain is initially set to $\gamma_{0.5\text{pop}} = 11.5 \text{ mN/m}$, then oscillates with an amplitude of 1% (corresponding to 2.35 mN/m), with a period of $T = 50 \text{ ms}$ (i.e., $10 \times \tau_{\text{max}}$ for these spandexes).

i.e., equally fast, which requires a transition barrier located halfway between CN and EX (Fig. 3). In this section (and in Fig. 4 B and Fig. 5) we therefore use a value A_* halfway between A_{CN} and A_{EX} .

Fig. 4 B illustrates the effectiveness of such a spandex with a sinusoidal applied strain centered at $\gamma_{0.5\text{pop}}$. Note how a spandex with a larger ΔA damps more effectively than another with a small ΔA . However, larger C_{prot} would increase the effectiveness of any spandex population (Fig. 5 A). At sufficiently high C_{prot} , even proteins with very small area expansion (e.g., KvAP with $\sim 1.5 \text{ nm}^2$) could serve as tension-damping spandex proteins. The maximum tension that could be relieved would, however, be small.

As seen in Fig. 5 B the bilayer tension oscillates with a large amplitude when strain oscillation period is short, and vice versa when it is long. The limit on the period below which

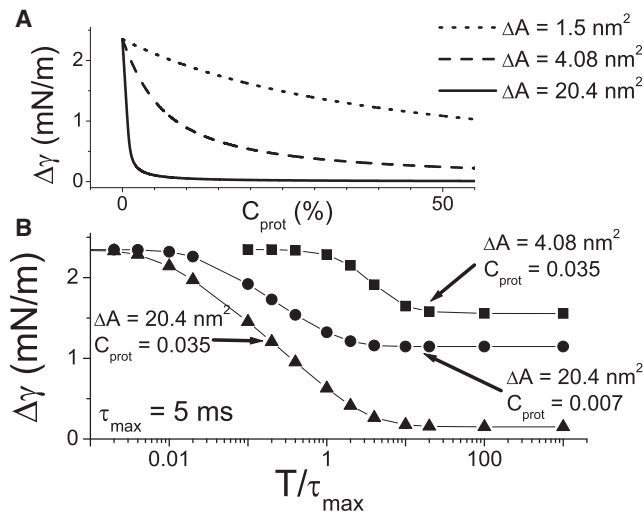


FIGURE 5 Damped tension excursions. (A) For a quasistatic strain oscillation, the amplitude of the tension variation, $\Delta\gamma$, for three different spandexes varies C_{prot} . (B) $\Delta\gamma$ varies with the period (T) of the oscillating strain (normalized to τ_{max}). For rapid oscillations (toward the *left*), tension damping is ineffective and the tension oscillation amplitude is that of the strain oscillation (multiplied by compressibility = 2.35 mN/m). For slow strain oscillations (toward the *right*), the effectiveness varies with C_{prot} and ΔA . In panels A and B, strain amplitude is 1% (corresponding to 2.35 mN/m). Plots were obtained by solving the model for different C_{prot} ; ΔA and T and are not analytic functions.

the tension oscillation amplitude, $\Delta\gamma$, is no longer damped is a function of both ΔA and C_{prot} . Fig. 5 B also shows how a large ΔA spandex protein is more effective than a smaller ΔA .

INTERACTING POPULATIONS

Bacterial osmovalve opening is best saved for near catastrophic bilayer strain, so a mechanism whereby the valve could ignore transiently increasing tension would be useful. Two populations of MS proteins, one acting as spandex, the other as osmovalve, could help ensure the osmovalve's appropriate deployment. The two populations could be different proteins, e.g., MscS-like proteins as spandex, MscL as osmovalve. Alternately, one protein modulated two ways might serve. In a MscS/MscL pairing, the MscS would need to expand to a nonpermeant state. In vitro, MscS exhibits three states: closed, open, and inactivated (20). MscS gating models based on high-resolution structure (47) indicate that conditions that increase the separation between TM3a (transmembrane helix regions whose rotations break a vapor lock to create a permeation path) should lead to more rapid inactivation. Perhaps in vivo bilayer chemistry provides such conditions. The transit from closed to inactivated (either directly or perhaps via a very short-lived open state) would be a MS expansion (19) and could allow MscS to serve as spandex. Though not seen in vitro for wild-type MscS, it seems plausible in vivo as it does occur in vitro for mutant MscS-G121A (20). Alternatively, closed-open would be a spandex transition if, in vivo, the permeation path was occluded.

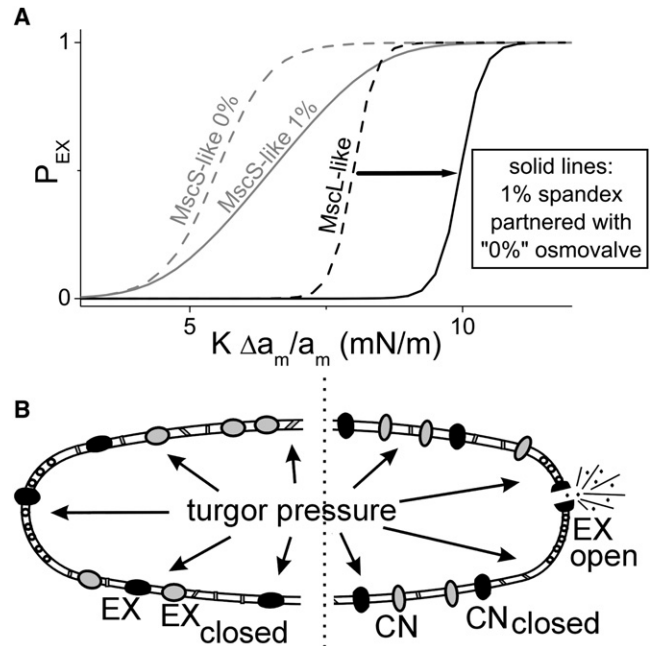


FIGURE 6 Spandex-osmovalve partnerships. (A) For a MscS-like spandex and a MscL-like osmovalve, dotted lines show isolated protein ($C_{\text{prot}} = 0$ Boltzmanns). If the membrane concentration of MscS-like spandex is increased to 1% (gray solid), this right-shifts the Boltzmann of the single MscL-like osmovalve (black solid). (B, left) differential modulation of a MscL population to yield a spandex/osmovalve duo. Anionic lipids positively influence stress-induced opening of MscL (53) and cardiolipin, an anionic negative curvature lipid, segregates to the poles of cylindrical bacteria (54). MscL is ubiquitously dispersed in bacterial membranes (55) (unlike pole-preferring osmotransporter, ProP (56)). If the polar chemical environment is needed for osmovalve opening and not for the preopening expansion, then MscL along the cylindrical surface of the bacterium could exclusively operate in spandex mode. Moreover, since Laplace's law dictates that tension in the cylinder would exceed that at hemispheres, spandex would respond before the polar osmovalves, thus preventing its unnecessary deployment (i.e., effectively right-shifting the MscL-osmovalve, as in panel A). Two spandexes are shown black for the modulated MscL and gray for different protein species to indicate that multiple spandex species (e.g., MscS-like proteins) could participate. (B, Right) If proteins in the cylindrical region were unable to expand, the full impact of increasing turgor pressure would be borne by one, or a few, polar osmovalve(s) that would expand, open, and dump osmolytes.

Consider two populations—a MscS-like spandex and a MscL-like osmovalve—of proteins in a bilayer subjected to a slow (quasistatic) increase of imposed strain that expands the MscS-like population but not the MscL-like osmovalve. This requires that the MscS-like spandexes have a (single protein) midpoint, $\gamma_{0.5}$, below that of the osmotic valve, and that its transition be sharp enough to expand all the spandex before the valve is deployed. For the MscL-like channel we re-use parameters from the previous sections, and for the MscS-like spandex we take its midpoint to be 5.5 mN/m, $\Delta A = 8.4 \text{ nm}^2$ (19), $A_{\text{CN}} = 10 \text{ nm}^2$.

Assuming a bacterium has only one (or a few) MscL multimers able to act as osmovalves, the $C_{\text{prot}} = 0\%$ case would approximate its cell-population response. Fig. 6 A shows the

behavior of an isolated MscL-like osmovalve on an imposed strain axis (due, say, to turgor pressures of various strengths). Also plotted are the spandex behaviors, first for the isolated protein case ($C_{\text{prot}} = 0\%$) and then for an upregulated population ($C_{\text{prot}} = 1\%$) of MscS-like spandex (this result was seen in Fig. 3). The new result here is as follows: in the presence of 1% MscS, the midpoint of the (isolated) MscL-like osmovalve shifts (its slope unchanged) to higher strains (i.e., higher turgor pressures). The critical point is that the osmovalve (the MscL-like protein) still opens at the same bilayer tension, but the system strain needed to achieve the appropriate tension is larger because part of the strain is absorbed by the expanding MscS-like spandex proteins. The need for a population of spandex could explain why low MscS levels, equivalent to the basal level of expression for low osmolarity exponential phase growth, are insufficient for osmoprotection (15).

Fig. 6 B depicts how the spandex-dependent MscL right-shift could operate in bacteria with (at least) one MscL-like osmovalve plus a population of either functional (*left*) or nonfunctional (*right*) spandex. The spandex could be MscS-like (*gray*) and/or MscL-like multimers (*black*) that can expand, but that do not open, due to modulation by spatially segregated bilayer constituents (see caption). Note how in this scenario, the bilayer mechano-chemical confinement of osmovalve-competent MscLs at the hemispherical region, plus operation of spandex in the chemically distinctive and more highly pressure-sensitive cylindrical regions, further enhances the valve/spandex partnership.

DISCUSSION

That membrane proteins with large Δ -area transitions can reversibly control cell shape is known (31); that large Δ -area transitions could also be exploited to reversibly control membrane tension is what we explore here. Bacteria, which have MS membrane proteins with exceptionally large Δ -area transitions (3), intermittently experience moderate to extreme osmotic perturbations. Some bacterial MS proteins expand at intermediate, others at near-lytic membrane tensions. For both, it is unclear why multiple copies are deployed and how/if they interact functionally. We explored how closed-closed spandex proteins modeled on bacterial MscL and MscS (or hypothetical nonpermeable variants) might prevent tension increases or maintain bilayer tension within particular ranges. In bacteria, regulation of bilayer tension by such spandex proteins could prevent cell rupture and/or unwarranted openings of osmovalves. In effect, expressed at sufficiently high density, MscL-like multimers capable of preopening spandex transitions should reduce their own use as osmolyte dumpers. For diverse proteins whose behavior changed with fluctuating tension (e.g., the voltage-gated channels of prokaryotic as well as eukaryotic cells) (39), damping spandexes could enhance tension stability.

To explore spandex membrane tension buffering, a model for spandex expansion/contraction kinetics was presented. Although consistent with previous MS membrane protein models (27,45,40–42,48,49), it includes only the energy contribution from area relaxation due to expanding proteins, with the energy barrier position made an explicit parameter. Tension-sensitive spandex kinetics revealed how the transition barrier position (A_*) dominates kinetics, without affecting the equilibrium. The model also reveals the consequence of an inherent negative feedback: insofar as a population of spandex proteins relieves bilayer tension upon expansion, it right-shifts its own effective midpoint tension as well as that for other MS proteins like osmovalves.

For optimal tension relief versus damping, spandexes of different properties are needed. To minimize osmovalve opening or forestall transient supralytic tensions, spandexes must act below these danger zones. During slow increases, tension rise stalls, thanks to spandex expansion. If tension did rise (e.g., during abrupt osmotic shocks), a spandex population would draw tension down toward the protein midpoint value. To ensure fast responses, A_* must be close to the A_{EX} .

In real MS proteins, A_* might be influenced by the stiffness of the protein states (45). A soft CN, stiff EX spandex would be an ideal tension reliever (A_* close to A_{EX}), and a spandex with equally stiff states, an ideal tension damper (A_* midway). A membrane protein's tertiary and quaternary structure determines its stiffness and allied mechanical properties. Insofar as spandex structure changed with different bilayer lipid species, covalent modifications, ionic environments etc., a cell might, to suit different needs, regulate the relative location of A_* in a given spandex. A single gene product might, thereby, provide for both tension relief and tension damping.

Spandex, if sufficiently abundant, shifts the midpoint tension of other proteins to higher tensions, possibly preventing them from expanding/opening. The spandex ΔA need not be particularly large. The condition to be obeyed is that the entire spandex population must expand before the event to be prevented could occur. This puts a condition on both the midpoint and ΔA (directly related parameters). In real cells and membranous organelles, high density proteins whose main functions are not to act as spandex but that happen to have Δ -area transitions, albeit small ones, might help preventing lytic tension increases.

Where spandexes serve to maintain a fixed bilayer tension, their midpoint must coincide with the system's target tension. A large ΔA spandex is most effective, but small ΔA spandex can suffice if present at high density. A large ΔA spandex is more effective in maintaining a target tension precisely; smaller ΔA spandexes allow deeper fluctuations. Another characteristic tension damper requirement, equally fast reactions to tension increases or decreases, is only possible with the transition barrier located midway between CN and EX. The [spandex] required depends on the strain level to be damped and spandex ΔA .

We finish by suggesting experimental approaches to explore spandex in cells and liposomes.

A fundamental system-level functional property of a spandex is its inherent negative feedback: as [spandex] increases, the system P_{EX} (strain) relation right-shifts and its slope flattens (see 0% vs. 1% plots for a MscS-like spandex, Fig. 6). With current signaling expansion, the closed-open expansion of MscS could be used to test this. MscS channels bioengineered to be photoinactivatable would be ideal (light would then lock-in their CN state). A giant protoplast with channels at high density (say approaching 1%) would be whole-cell clamped using a slow pressure ramp to strain the bilayer and yield a P_{EX} (strain) relation. Part of the population would then be photoinactivated, a new P_{EX} (strain) relation would be obtained, and so on, until one functional channel (0%) was tested. Or, more prosaically, with protoplast volume accurately measured, one could do among-protoplast comparisons of P_{EX} (strain) for WT channels at densities from very high down to 0%; such data might already be extant.

The other class of dose-response predictions of Fig. 6 (strain right-shift of MscL activation with increasing (MscS-like) [spandex]) should, in principle, be testable in MscS-and-MscL spheroplasts under whole-cell clamp (applied pipette pressure would constitute applied strain) by monitoring the output of an exquisitely sensitive pressure servo. Existing devices are designed for speed (e.g., (50)), but redesign for sensitivity seems feasible. During a slow volume (pressure) ramp in the absence of spandex, the output of the servo as a function of time should be a straight sloped line. With spandex present, the pressure servo output would at some point increase until all the spandex was deployed (response steepness would increase with increasing ΔA , and total deflection would be proportional to [spandex]) then resume increasing linearly in parallel to the no-spandex line (Fig. 2 C). MscL current turn-on would occur later and later (apparent right-shift) with more and more spandex.

AFM (33) might be able to detect tension relief and tension damping due to spandex events. With bacterial spheroplasts of known diameter, whole-cell clamped (isotonic solutions, fixed voltage, known pipette pressure) current would give the time course of osmovalve openings, while cell size nano-variations were followed by AFM in constant force mode. The latter would reflect bilayer tension changes, i.e., spandex activity. The temporal relationship between tension and current fluctuations (with flux effects compensated) would give a picture of the spandex behavior of the MS proteins (e.g., MscL, MscS, or their mutants).

To test for spandex-dependent osmo-mechano-protection, liposomes or bacteria under mechanical strain (osmotic downshock, fluid turbulence) could be used. One approach: reconstitute a spandex(es) (e.g., WT-MscL, which has a preopening spandex transition; MscS-G121A, which expands from closed to inactivated) at reasonably high density into small liposomes preloaded with two fluoro-tracers (one too large to permeate open MscS or MscL and one that permeates

the channel). The spandex would require a cysteine, endogenous or mutated into the protein, as inaccessible to the exterior medium except upon expansion, when a traceable sulfhydryl reagent present only in the bath would bind. Spandex should extend the strain range over which liposomes release neither of the aqueous tracers, and progressive [spandex] increases should progressively extend the strain range over which spandex-cysteine modification occurs without release of aqueous tracers. Live cell tests of bacteria overexpressing recombinant spandexes could combine cysteine-accessibility assays with viability assays (e.g., (14, 51)).

Engineered spandex proteins might be useful in the context of circulating drug delivery liposomes (52) that encounter transient, potentially lytic osmotic and shear forces.

SUPPORTING MATERIAL

An appendix with four figures is available at [http://www.biophysj.org/biophysj/supplemental/S0006-3495\(09\)01447-7](http://www.biophysj.org/biophysj/supplemental/S0006-3495(09)01447-7).

This work was funded by grants from the Natural Sciences and Engineering Research Council of Canada to B.J., and from the Heart and Stroke Foundation, Ontario, and the Canadian Institutes of Health Research to C.E.M.

REFERENCES

1. Hamill, O. P. 2006. Twenty odd years of stretch-sensitive channels. *Pflügers Arch. Eur. J. Phys.* 453:333–351.
2. Sukharev, S. I., and A. Anishkin. 2004. Mechanosensitive channels: what can we learn from “simple” model systems? *Trends Neurosci.* 27:345–351.
3. Booth, I. R., M. D. Edwards, S. Black, U. Schumann, and S. Miller. 2007. Mechanosensitive channels in bacteria: signs of closure? *Nat. Rev. Microbiol.* 5:431–440.
4. Corry, B., and B. Martinac. 2008. Bacterial mechanosensitive channels: experiment and theory. *Biochim. Biophys. Acta Biomembr.* 1778:1859–1870.
5. Evans, E., V. Heinrich, F. Ludwig, and W. Rawicz. 2003. Dynamic tension spectroscopy and strength of biomembranes. *Biophys. J.* 85: 2342–2350.
6. Sens, P., and M. S. Turner. 2006. Budded membrane microdomains as tension regulators. *Phys. Rev. E.* 73:31918.
7. Morris, C. E. 2002. How did cells get their size? *Anat. Rec.* 268: 239–251.
8. Sukharev, S. I., S. R. Durell, and H. R. Guy. 2001. Structural models of the MscL gating mechanism. *Biophys. J.* 81:917–936.
9. Reference deleted in proof.
10. Häse, C. C., R. F. Minchin, A. Kloda, and B. Martinac. 1997. Cross-linking studies and membrane localization and assembly of radiolabeled large mechanosensitive ion channel (MscL) of *Escherichia coli*. *Biochem. Biophys. Res. Commun.* 232:777–782.
11. Booth, I. R., M. D. Edwards, S. Black, U. Schumann, W. Bartlett, et al. 2007. Physiological analysis of bacterial mechanosensitive channels. *Methods Enzymol.* 428:47–61.
12. Batiza, A. F., M. M. C. Kuo, K. Yoshimura, and C. Kung. 2002. Gating the bacterial mechanosensitive channel MscL in vivo. *Proc. Natl. Acad. Sci. USA.* 99:5643–5648.
13. Perozo, E. 2006. Gating prokaryotic mechanosensitive channels. *Nat. Rev. Mol. Cell Biol.* 7:109–119.
14. Levina, N., S. Töttemeyer, N. R. Stokes, P. Louis, M. A. Jones, et al. 1999. Protection of *Escherichia coli* cells against extreme turgor by

- activation of MscS and MscL mechanosensitive channels: identification of genes required for MscS activity. *EMBO J.* 18:1730–1737.
15. Stokes, N. R., H. D. Murray, C. Subramaniam, R. L. Gourse, P. Louis, et al. 2003. A role for mechanosensitive channels in survival of stationary phase: regulation of channel expression by RpoS. *Proc. Natl. Acad. Sci. USA.* 100:15959–15964.
 16. Perozo, E., A. Kloda, D. M. Cortes, and B. Martinac. 2002. Physical principles underlying the transduction of bilayer deformation forces during mechanosensitive channel gating. *Nat. Struct. Mol. Biol.* 9: 696–703.
 17. Chiang, C. S., A. Anishkin, and S. Sukharev. 2004. Gating of the large mechanosensitive channel in situ: estimation of the spatial scale of the transition from channel population responses. *Biophys. J.* 86: 2846–2861.
 18. Hille, B. 1984. *Ionic Channels of Excitable Membranes.*, Vol. 174. Sinauer, Sunderland, MA.
 19. Sukharev, S. I. 2002. Purification of the small mechanosensitive channel of *Escherichia coli* (MscS): the subunit structure, conduction, and gating characteristics in liposomes. *Biophys. J.* 83:290–298.
 20. Akitake, B., A. Anishkin, N. Liu, and S. I. Sukharev. 2007. Straightening and sequential buckling of the pore-lining helices define the gating cycle of MscS. *Nat. Struct. Mol. Biol.* 14:1141–1149.
 21. Jackson, M. B. 2006. *Molecular and Cellular Biophysics.* Cambridge University Press, Cambridge, UK.
 22. Rawicz, W., K. C. Olbrich, T. McIntosh, D. Needham, and E. Evans. 2000. Effect of chain length and unsaturation on elasticity of lipid bilayers. *Biophys. J.* 79:328–339.
 23. Beveridge, T. J. 1988. The bacterial surface: general considerations towards design and function. *Can. J. Microbiol.* 34:363–372.
 24. Koch, A. L., and S. Woeste. 1992. Elasticity of the sacculus of *Escherichia coli*. *J. Bacteriol.* 174:4811–4819.
 25. Pelling, A. E., S. Sehati, E. B. Gralla, J. S. Valentine, and J. K. Gimzewski. 2004. Local nanomechanical motion of the cell wall of *Saccharomyces cerevisiae*. *Science.* 305:1147–1150.
 26. Callaway, E. 2008. Cell biology: bacteria's new bones. *Nature.* 451: 124–126.
 27. Sukharev, S. I., W. J. Sigurdson, C. Kung, and F. Sachs. 1999. Energetic and spatial parameters for gating of the bacterial large conductance mechanosensitive channel, MscL. *J. Gen. Physiol.* 113: 525–540.
 28. Hudspeth, A. J. 2008. Making an effort to listen: mechanical amplification in the ear. *Neuron.* 59:530–545.
 29. Mio, K., Y. Kubo, T. Ogura, T. Yamamoto, F. Arisaka, et al. 2008. The motor protein prestin is a bullet-shaped molecule with inner cavities. *J. Biol. Chem.* 283:1137–1145.
 30. Adachi, M., and K. H. Iwasa. 1999. Electrically driven motor in the outer hair cell: effect of a mechanical constraint. *Proc. Natl. Acad. Sci. USA.* 96:7244–7249.
 31. Zheng, J., W. Shen, D. Z. Z. He, K. B. Long, L. D. Madison, et al. 2000. Prestin is the motor protein of cochlear outer hair cells. *Nature.* 405: 149–155.
 32. Lecar, H., and C. E. Morris. 1993. *Biophysics of mechanotransduction. In Mechanoreception by the Vascular Wall.* Futura Publications, Mount Kisco, NY.
 33. Beyder, A., and F. Sachs. 2009. Electromechanical coupling in the membranes of *Shaker*-transfected HEK cells. *Proc. Natl. Acad. Sci. USA.* 106:6626–6631.
 34. Laitko, U., and C. E. Morris. 2004. Membrane tension accelerates rate-limiting voltage-dependent activation and slow inactivation steps in a *Shaker* channel. *J. Gen. Physiol.* 123:135–154.
 35. Ospeck, M., X. Dong, and K. H. Iwasa. 2003. Limiting frequency of the cochlear amplifier based on electromotility of outer hair cells. *Biophys. J.* 84:739–749.
 36. Lamb, T. D., and E. N. Pugh. 2004. Dark adaptation and the retinoid cycle of vision. *Prog. Retin. Eye Res.* 23:307–380.
 37. Teller, D. C., T. Okada, C. A. Behnke, K. Palczewski, and R. E. Stenkamp. 2001. Advances in determination of a high-resolution three-dimensional structure of rhodopsin, a model of G-protein-coupled receptors (GPCRs). *Biochemistry.* 40:7761–7772.
 38. Marsh, D. 2007. Lateral pressure profile, spontaneous curvature frustration, and the incorporation and conformation of proteins in membranes. *Biophys. J.* 93:3884–3899.
 39. Morris, C. E., and P. F. Juranka. 2007. Lipid stress at play: mechanosensitivity of voltage-gated channels. *Curr. Top. Membr.* 59:297–337.
 40. Reeves, D., T. Ursell, P. Sens, J. Kondev, and R. Phillips. 2008. Membrane mechanics as a probe of ion-channel gating mechanisms. *Phys. Rev. E.* 78:041901.
 41. Wiggins, P., and R. Phillips. 2004. Analytic models for mechanotransduction: gating a mechanosensitive channel. *Proc. Natl. Acad. Sci. USA.* 101:4071–4076.
 42. Wiggins, P., and R. Phillips. 2005. Membrane-protein interactions in mechanosensitive channels. *Biophys. J.* 88:880–902.
 43. Phillips, R., T. Ursell, P. Wiggins, and P. Sens. 2009. Emerging roles for lipids in shaping membrane-protein function. *Nature.* 459:379–385.
 44. Ursell, T., K. C. Huang, E. Peterson, and R. Phillips. 2007. Cooperative gating and spatial organization of membrane proteins through elastic interactions. *PLoS Comput. Biol.* 3:803–812.
 45. Sukharev, S. I., and V. S. Markin. 2001. Kinetic model of the bacterial large conductance mechanosensitive channel. *Biologiëskie Membrany.* 18:440–445.
 46. Boucher, P. A., B. Joós, M. J. Zuckermann, and L. Fournier. 2007. Pore formation in a lipid bilayer under a tension ramp: modeling the distribution of rupture tensions. *Biophys. J.* 92:4344–4355.
 47. Wang, W., S. S. Black, M. D. Edwards, S. Miller, E. L. Morrison, et al. 2008. The structure of an open form of an *E. coli* mechanosensitive channel at 3.45 Å resolution. *Science.* 321:1179–1183.
 48. Markin, V. S., and F. Sachs. 2004. Thermodynamics of mechanosensitivity. *Phys. Biol.* 1:110–124.
 49. Hamill, O. P., and B. Martinac. 2001. Molecular basis of mechanotransduction in living cells. *Physiol. Rev.* 81:685–740.
 50. Besch, S. R., T. Suchyna, and F. Sachs. 2002. High-speed pressure clamp. *Pflügers Arch. Eur. J. Phys.* 445:161–166.
 51. Anishkin, A., V. Gendel, N. A. Sharifi, C. S. Chiang, L. Shirinian, et al. 2003. On the conformation of the COOH-terminal domain of the large mechanosensitive channel MscL. *J. Gen. Physiol.* 121:227–244.
 52. Zhu, T. F., and J. W. Szostak. 2009. Preparation of large monodisperse vesicles. *PLoS One.* 4:e5009.
 53. Powl, A. M., J. M. East, and A. G. Lee. 2008. Anionic phospholipids affect the rate and extent of flux through the mechanosensitive channel of large conductance MscL. *Biochemistry.* 47:4317–4328.
 54. Mukhopadhyay, R., K. C. Huang, and N. S. Wingreen. 2008. Lipid localization in bacterial cells through curvature-mediated microphase separation. *Biophys. J.* 95:1034–1049.
 55. Norman, C., Z. W. Liu, P. Rigby, A. Raso, Y. Petrov, et al. 2005. Visualization of the mechanosensitive channel of large conductance in bacteria using confocal microscopy. *Eur. Biophys. J.* 34:396–402.
 56. Romantsov, T., Z. Guan, and J. M. Wood. 2009. Cardiolipin and the osmotic stress responses of bacteria. *Biochim. Biophys. Acta.* 1788:2092–2100.